A REVIEW OF HIGH POWER OPCPA TECHNOLOGY FOR HIGH REPETITION RATE FREE-ELECTRON LASERS*

M. J. Prandolini†, R. Riedel, Helmholtz-Institut Jena, Fröbelstieg 3, D-07743 Jena, Germany
M. Schulz, Deutsches Elektronen-Synchrotron DESY, Notkestrasse 85, D-22607 Hamburg, Germany
F. Tavella‡, SLAC National Accelerator Laboratory, 2575 Sand Hill Rd., CA 94025, USA

Abstract

High repetition rate free-electron lasers (FEL) require the development of new laser systems that have the ability to operate at high average power. Optical parametric chirped-pulse amplification (OPCPA) is presently the most promising method to fulfill these requirements. This technique has been used to demonstrate amplification up to tens of watts with a repetition rate in the range between tens of kHz to MHz in burst and continuous mode. We review the current OPCPA technology for systems operating around 800 nm; this includes various frontend options, pump amplifier technology and latests results, and we discuss the important requirements for achieving high power lasers in both burst and continuous operation.

INTRODUCTION

High repetition rate FELs present some unique challenges for laser developers. Superconducting cavities, developed at DESY [1], allow a much higher repetition rate than conventional accelerator technologies; however, they have a burst mode structure. For example, FLASH at Hamburg has a maximum repetition rate of 1 MHz within a burst structure of 800 µs at 10 Hz [2, 3]. This presents major challenges for the design and operation of FEL seeding and pump-probe lasers operating in burst mode. At lower repetition rates, conventional Ti:sapphire lasers are currently used in FELs [4]. However, in the last years there has been remarkable progress in high average power OPCPA systems (Fig. 1). Currently, the high repetition rate and high power OPCPAs have been demonstrated at an average power of 11.4 W at 3.25 MHz [5] and 22 W at 1 MHz [6], and in a burst operation of 38.5 W at 27.5 kHz within a burst structure similar to FLASH [7]. For the amplification of high power, few-cycle, optical pulses, OPCPA is the leading technology [6, 8–10], due to the inherent bandwidth limitations of Ti:saphire technology [11].

A comparison of a Ti:sapphire amplifier and a noncollinear optical parametric amplifier (OPA) is schematically shown in Fig. 2. In a Ti:sapphire amplifier, the pump pulses are used to create a population inversion, where the pump energy is stored in the gain material itself before being transfered to the signal via stimulated emission. The quantum defect for Ti:sapphire is 34%, the resulting energy difference

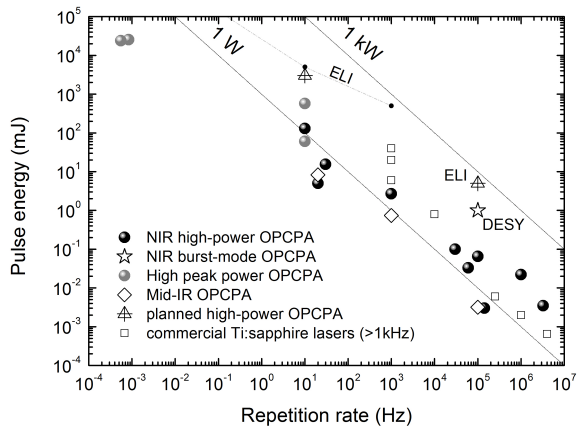

Figure 1: Current and planned high average power laser systems: ELI - Extreme Light Infrastructure; DESY - Deutsches Elektronen-Synchrotron

goes into heating of the gain material, which therefore has to be cooled. In contrast in a noncollinear OPA, the energy of the pump wave (ω_P) is transferred, via a second order nonlinear effect within the gain material, into signal (ω_S) and idler (ω_I) waves. Thereby, energy conservation is maintained between the three waves ($\omega_I = \omega_P - \omega_S$). For certain applications the idler wave can be used, but in general it is discarded. Nevertheless, a small amount of linear absorption from the pump, signal and idler does occur, which starts to become noticeable at around tens of watts of output energy.

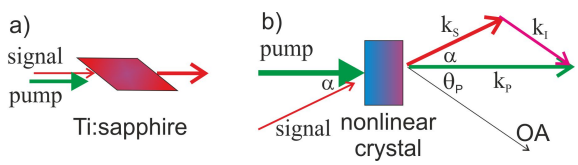

Figure 2: A comparison of laser amplifier technologies: (a) The Ti:sapphire amplifiers operate using the conventional population inversion within the gain material created by a pump pulse. (b) In noncollinear OPA, the energy of the pump is transferred, via a second order nonlinear effect within the gain material, into signal and idler waves: α - non-collinear angle; θ_P - angle between the pump wavevector (k_P) and the optical axis (OA); k_S and k_I - wavevectors of the signal and idler, respectively.

* Work supported by the Helmholtz Institute Jena and the Deutsches Elektronen-Synchrotron DESY in Hamburg. The authors would also like to thank the Helmholtz Association for their support for the spin-off project *Class 5 Photonics*.
† mark.prandolini@desy.de
‡ Formally at DESY

ISBN 978-3-95450-133-5

Another important concept is the use of chirped-pulsed amplification (CPA). In CPA, the signal pulses are first temporally stretched to obtain lower signal intensities before being amplified, thereafter the signal pulses must be compressed. This technique lowers the peak intensity during the amplification phase in order to avoid nonlinear propagation effects and material damage issues. The first realization of an optical parametric chirped-pulse amplifier (OPCPA) was performed by Dubietis et al. [12] in 1992. It was recognized quite early that OPCPA has the potential to overcome the limitations imposed on conventional laser amplifier technologies (Ross et al. [13]). Reviews of the progress are given in [14–16]

This remarkable progress has been made possible through the development of high average power pump amplifier technology. Pump pulse durations should ideally be in the sub/few picosecond range providing tens to hundreds of millijoules of energy. Short pump pulses not only reduce the required stretching and compression of the ultrabroadband signal pulse, but also allow for higher pump intensities in the nonlinear crystals before the damage threshold is reached [17]. These laser parameters can potentially be achieved using Yb-doped solid-state laser technology. A typical system usually consists of a Yb-doped fiber amplifier as a frontend combined with, for example, a Yb:YAG (YAG – yttrium aluminium garnet) Innoslab amplifier system [18] and/or a Yb:YAG thin-disk amplifier for low gain, high average power amplification [19]. Presently, commercial OPCPA-pump amplifiers operating in the tens of kilowatt level do not exist, but are planned for the near future. In the design of an ultrabroadband, high power OPCPA system, the OPCPA-pump will be the most costly and energy consuming part of the system. Therefore, the design of an OPCPA should try to optimize the use of the available pump energy. This also keeps initial and running costs to a minimum, and additionally, by reducing the total pump power requirements, the total thermal load and heat dissipation are also minimized.

The outline of this review is as follows. First a general layout of an OPCPA system is discussed, including various frontend options. Then pump amplifier technologies are discussed. Thereafter a review of the OPCPA methods for systems around 800 nm are discussed, including typical nonlinear crystals, thermal effects and a selection of results from both burst and continuous mode OPCPA.

GENERAL LAYOUT AND OPCPA FRONTENDS

The general layout of a high repetition rate OPCPA is shown in Fig. 3. It consists of a frontend, which supplies a narrow band OPCPA-pump pulse (centered at 1030 nm) to the Yb-doped OPCPA-pump system and a broadband signal pulse (centered at 800 nm) to be amplified. In the case shown in Fig. 3, the frontend is a Ti:Sa oscillator, which has enough energy at 1030 nm to simultaneously seed both pump and OPCPA systems. In this example, both the pump and signal

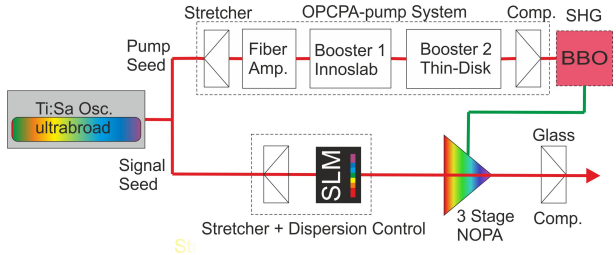

Figure 3: Layout of an OPCPA: Osc. - Laser Oscillator; SLM - spatial light modulator; Comp. - optical compressor; SHG - second harmonic generation; NOPA - non-collinear optical parametric amplifier; BBO - β-barium borate (BaB_2O_4), an example of a nonlinear doubling crystal.

pulses undergo CPA. The OPCPA-pump system consists of a stretcher and a number of amplifier stages (discussed in the next section) followed by second harmonic generation (SHG) to produce pump pulses at 515 nm. Typical SHG nonlinear doubling crystals at these wavelengths are BBO – β-barium borate or LBO – lithium triborate. On the signal side, the signal seed requires a careful dispersion management. In the case shown in Fig. 3, the pulses are first stretched with negative dispersion, so that they match the pulse duration of the pump pulse. Additionally, for short pulses (below 10 fs) the phase of the pulses can be modified by a spatial light modulator (SLM). Thereafter the signal pulses are amplified in a three stage non-collinear OPA. Finally, a compressor consisting of glass and if necessary chirped mirrors is used to produce Fourier-limited pulses.

OPCPA Frontends

The aim of the frontend is to provide a broadband seed pulse to the non-collinear OPA stages centered at 800 nm and a narrow band seed pulse to the OPCPA-pump system at 1030 nm. One possibility would be to use two (master and slave) oscillators electronically (or optically) synchronized together; however, this arrangement not only increases the complexity of the setup, it also adds jitter between OPCPA-seed and OPCPA-pump pulses at the non-collinear OPA stages. This is particularly critical when using Yb-YAG technology, where the pump pulse durations are usually below 1 ps. A better arrangement would be to use a single oscillator to seed both simultaneously, as shown in Fig. 3. Commercial, ultrabroadband, Ti:Sa oscillators centered at 800 nm now exist, where there is enough energy at the pump wavelength of 1030 nm so that it can be filtered out and used as the pump seed pulse (for example, see Venteon Laser Technologies GmbH). If the Ti:Sa oscillator does not have enough energy at the pump wavelength, a fraction of the oscillator pulses can be coupled into a photonic crystal fiber (for example, 20 cm long NKT NL-890 nm) and frequency shifted to the Yb-gain region, as was done in [6,9]. However, this option adds complexity and adds potential long-term instability to the system. In general, the stability of commerical, ultrabroadband Ti:Sa oscillators has greatly improved in the last years. For ultrashort pulses and in cases which

ISBN 978-3-95450-133-5

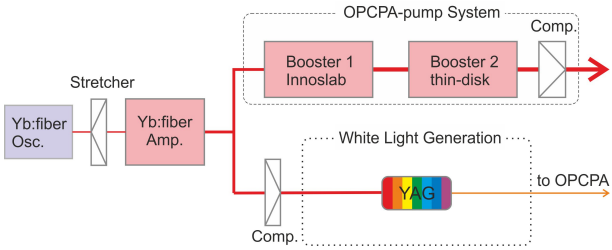

Figure 4: Frontend of an OPCPA using Yb:fiber oscillator (Onefive GmbH) to seed a Yb:fiber amplifier (Active Fiber Systems GmbH), which is used as seed for both the OPCPA-pump system and the dedicated WLG.

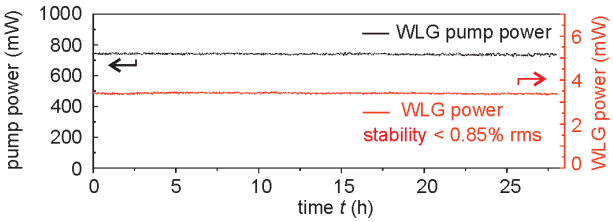

Figure 5: Stability test of the WLG: pump power (black) and WLG power (red), measured over 28 hours. The investigated WLG spectral region ranged from 650 nm to 950 nm.

require carrier envelope phase (CEP) stability, CEP stable Ti:Sa oscillators are still a viable option for OPCPA frontends. However, for maintenance-free, continuous operation over days other options can be explored.

White light continuum generation (WLG), based on "turnkey", stable fiber lasers, is one potential frontend solution for providing maintenance-free, continuous operation [7, 18]. YAG crystals have been extensively tested at these wavelengths for generating OPCPA seed signals [7, 18]. Other host materials have been reviewed in [20]. YAG requires pulse durations below 1 ps and pulse energies between 1-10 µJ, depending on the experimental conditions [18]. Depending on the exact details of the stretcher/compressor OPCPA-pump system and/or the stability of the booster amplifiers, a fraction of the pump pulse can be used for WLG.

Another possibility would be to use a dedicated WLG using a stable fiber amplifier, with a compacter stretcher/compressor configuration. An example is shown in Fig. 4, where a Yb:fiber oscillator is used to seed a fiber amplifier providing both the OPCPA-pump seed and a dedicated WLG seed. This system was extensively tested in continuous mode [7] and was shown to have good stability over days of operation (Fig. 5).

PUMP AMPLIFIER TECHNOLOGIES

High power, ultrabroadband OPCPA currently use pump amplifier technologies based on Yb-doped solid-state amplifiers, which support a larger bandwidth, and therefore shorter pulses, compared to Nd-doped laser systems. Short pump pulses are important because the amplification of ultrabroadband signal pulses requires high pump intensities in the OPCPA nonlinear crystals. The damage threshold scales proportional to $\sqrt{\tau}$ with slight deviation from this scaling below 20 picoseconds [17]; for slightly below 1 ps this scaling factor can be considered as a upper limit. Therefore the intensity at which damage occurs scales as $\sim 1/\sqrt{\tau}$.

The CPA is the basis of all OPCPA-pump amplifier technologies, and is used for similar reasons as discussed above for OPCPA. Another important aspect of high average power systems is thermal management. Presently, there are three types of technologies, with three different corresponding geometries, that dissipate the high thermal load in the gain materials. First, Yb-doped rod-type fiber amplifier systems can reach kW-level but are limited in pulse energy extraction [21]. This boundary can be overcome by coherently combining individually cooled fiber rods [22]. Second, slab type geometries can be used, such as Innoslab technology [23]. In this case, cooling occurs on both sides of the slab (gain material) resulting in thermal lensing for the beam propagating between the walls of the cooling surfaces; this effect is used as an integral part of the pulse propagation. Third, thin-disk amplifiers cool only on one side of a thin disk [24]; the pump seed propagates perpendicular to the surface of the thin disk and is reflected on the heat sink. This geometry avoids thermal lensing, if the disk is thin compared to its diameter, but results in a small gain per single pass. The latter two technologies can potentially reach the multi-kW-level at high pulse energies without the need to coherently combine.

In our work, we have combined all three technologies, for example a fiber amplifier can be used as a seed for further amplification with a single stage thin-disk amplifier, or with a combined Innoslab and thin-disk amplifiers. Our OPCPA-pump development concentrated on thin-disk multipass amplifiers, as this technology offers the best possibility for both high energy as well as high power scaling. In an initial development, we have demonstrated kilowatt level output powers in a single stage thin-disk multipass amplifier, in the burst operation mode [19]. This was achieved with a 50 W fiber amplifier (Helmholtz Institute Jena) and optionally a 500 W Innoslab amplifier (AMPHOS GmbH) as seed source for the thin-disk multipass amplifier. The thin-disk amplifier head was provided by TRUMPF GmbH + Co. KG.

In a second setup, a total output power of 14 kW was achieved in a burst operation mode from a 2-stage cascaded Yb:YAG thin-disk multipass amplifier [25]. This yielded a pulse energy of 140 mJ at 100 kHz in burst mode. A block diagram of the pump amplifier setup is shown in Fig. 6a. The seed for the entire amplifier system was generated in a 10 W fiber amplifier system. This was further amplified in an Innoslab amplifier with 500 W output power and a subsequent Innoslab booster amplifier with 1.5 kW output power. After spatial filtering, a total intra-burst output power of 1 kW could be used to seed the thin-disk amplifiers. The multipass setups were conceived for 7 passes through each amplifier. In the first thin-disk amplifier, an output burst energy of 5.4 J was achieved, corresponding to an intra-burst output power of 7 kW. The second thin-disk amplifier increased the output burst energy to 11.2 J, which corresponds to an intra-

ISBN 978-3-95450-133-5

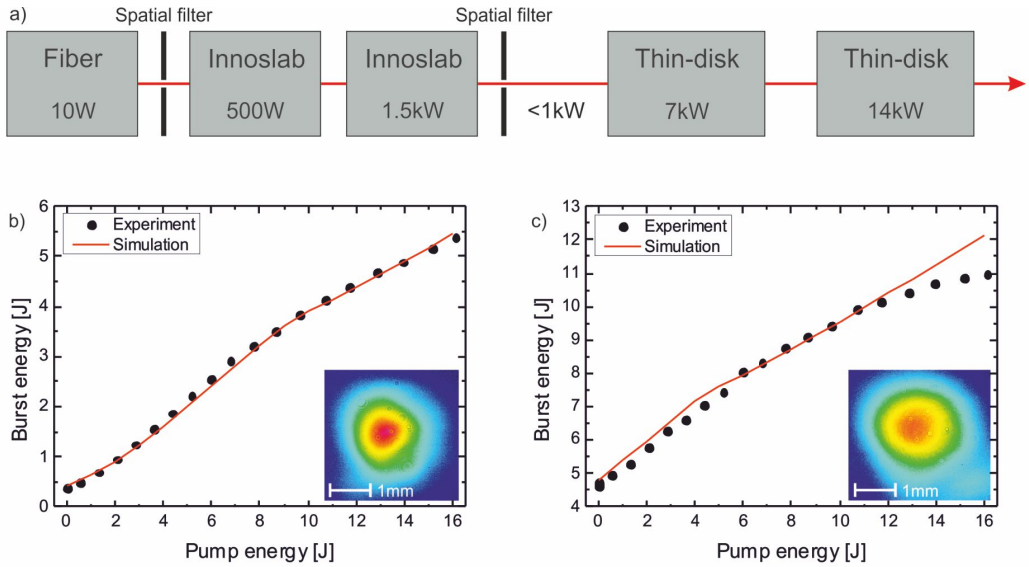

Figure 6: (a) Block diagram of the amplifier setup with a fiber amplifier as seed source for further amplification with two Innoslab booster stages and two thin-disk stages. Experimental (black) and simulated (red) characteristics of the thin-disk amplifier for b) the first amplifier stage and c) the second amplifier stage.

burst output power of 14 kW. The resulting energetics of the two thin-disk amplifiers with analytical simulations are displayed together with the output beam profiles in Fig. 6b and Fig. 6c. Additionally, the spectral bandwidth of the output pulses supports compression to pulse durations below one picosecond. These pulse properties make the amplifier system very interesting as a pump amplifier for a high energy, high repetition rate OPCPA system.

The above mentioned thin-disk amplifier development was carried out in a burst mode operation, which was dictated by the burst structure of the FEL pulse train using superconducting acceleration cavities. This creates both new challenges and benefits. In general, the most important problem to solve with high average power lasers is the induced heat load. However, burst-mode laser amplifiers combine high pulse energies at high repetition rates with the low average power on the sample due to a low duty cycle. Thus, a high thermal load on the sample can be avoided keeping the beneficial effect of the high intra-burst power. The challenges with burst mode amplifiers is providing a 'flat' burst profile, with respect to pump-pulse characteristics, over the selected signal pulses to be amplified. To create a flat burst requires a delicate balance of the timing between the arrival time of the seed pulses and the timing of the diode pulses [19]. In the case of the Innoslab amplifier, we have observed a small pointing error and beam profile deviations within the first ~100 µs of the burst. This results from the time required to form a stable thermal lensing for correct beam propagation within the amplifier.

There is currently rapid progress with all three technologies and commercial options exist for moderate power levels. We have made a subjective comparison between the various pump technologies (Table 1), with the restriction that coherent combining for rod-type fiber systems was not considered and the multipass thin-disk was not optimized for stability [25]: for example, no relay imaging was used and the amplifier was not in a sealed environment.

Table 1: Comparison of Three Types of Pump Amplifiers: rod-type fiber, Innoslab and multipass thin-disk amplifiers (++ very good; + good; ∘ average; − poor; −− very poor).

	Fiber	Innoslab	Thin-Disk
Average Power	∘	++	++
Pulse Energy	∘	+	++
Single Pass Gain	++	+	−−
Pointing Stability	++	+	−
Energy Scaling	−−	+	++

OPTICAL PARAMETRIC CHIRPED-PULSE AMPLIFICATION (OPCPA)

At the core of an OPCPA system is the optical parametric amplification (OPA). OPA is related to difference frequency generation (DFG), where a three wave mixing process takes place in an optical crystal as a second-order nonlinear effect. At the wavelengths considered here, the material response to a nonlinear optical excitation is instantaneous. Figure 2b shows the principle of non-collinear three wave mixing, which involves a strong pump wave, a signal wave and a third wave, the idler. The pump, signal and idler waves must firstly fulfill the energy conservation condition, $\omega_I = \omega_P - \omega_S$, where the suffixes P, S and I refer to pump, signal and idler waves, respectively. A second important condition is momentum conservation (or the phase matching condition): $\delta\mathbf{k}(\theta_P, \lambda_P, \lambda_S) = \mathbf{k}_P(\theta_P, \lambda_P) - \mathbf{k}_S(\lambda_S) - \mathbf{k}_I$.

ISBN 978-3-95450-133-5

Table 2: Properties of Nonlinear Crystals: d_{eff} effective nonlinear optical coefficient, ρ walk-off angle, TT temperature tolerance, AT angular tolerance. Values given for $\lambda_{\text{pump}} = 515$ nm and $\lambda_{\text{signal}} = 800$ nm. These values are taken from [26].

	d_{eff} [pm/V]	ρ [mrad]	TT [K cm]	AT [mrad cm]
BBO	2.0	55.8	39.7	0.56
LBO	1.0	7.06	6.8	4.54
BIBO	3.0	25.0	2.74	1.15
YCOB	0.36	32.1	110.9	0.94

In high power applications, the pump is narrow band and it is desirable to amplify a broadband signal. Therefore, for a fixed λ_P, there is generally one combination of θ_P and λ_S that satisfies the phase matching condition exactly (i.e. $\delta\mathbf{k} = 0$). To achieve broadband phase matching, and therefore broadband amplification, another parameter needs to be introduced. One option is to introduce a non-collinear angle (α) between the pump and signal [15]. Additionally, the gain bandwidth ($\Delta\nu$) also depends on the crystal length L, the pump intensity I_P and the effective nonlinear coefficient d_{eff}:

$$\Delta\nu = 0.53\sqrt{\Gamma/L}\;|\,u_{SI}\,|\,/c, \tag{1}$$

where $1/u_{SI} = 1/u_S - 1/u_I$ is the group-velocity mismatch between the signal and idler pulses and the gain Γ is given by

$$\Gamma = d_{\text{eff}}\sqrt{\frac{2\omega_S\omega_I I_P}{\epsilon_0 n_S n_I n_P c^3}}. \tag{2}$$

Therefore, additional conditions to achieve broadband signal pulses are short nonlinear crystals and high pump intensities.

For high power applications centered at 800 nm, β-barium borate (BBO) and lithium triborate (LBO) are well-established materials [26, 27], which are used in the OPCPA of ultrabroadband, high repetition rate lasers. Other crystals worth mentioning are bismuth triborate (BIBO) and yttrium calcium oxyborate (YCOB) [28]. A summary of some important parameters is given in Table 2. Compared to BBO and LBO, BIBO has a larger nonlinear coefficient (d_{eff}), but also has significant nonlinear absorption at 515 nm [27], making it unsuitable for high power applications. YCOB is presently not commercially available. It has a smaller nonlinear coefficient and the gain bandwidth is not as large as BBO and LBO. But because its temperature tolerance is large (Table 2) and therefore insensitive to temperature changes, it might be useful for narrow band, high power applications.

The aim of the dispersion management is to achieve maximum OPA efficiency of the signal pulse, by temporally stretching the signal pulse to match the pump pulse. Thereafter, the signal pulses must be compressed to their Fourier-limit. Compared to older OPCPA systems based on Nd-doped amplifiers, Yb:YAG offers much shorter pump pules, and therefore, the required matching signal stretcher/compressor pairs are compacter, making a smaller footprint on the optical table and increasing the overall stability. The signal pulses can be stretched using a prism pair [7] (chirped mirrors are also an option). After amplification the pulses can be compressed in glass. For signal pulses under 10 fs, it is necessary to control the higher order dispersion using an SLM as shown in Fig. 3.

For high power (mJ pulse energy) OPCPA applications, a three stage OPCPA setup is generally optimal (Fig. 7). The first stage brings the signal pulses from the nJ to the µJ level. This reduces the amplified parametric fluorescence in the second and third stages, where more than 90% of the pump energy is used [7]. The gain in this first stage is between 10^4 and 10^5. The next two stages provide gain in the range 50-100 and 2 for the second and third stages, respectively. An example of a three-stage broadband amplification of a 800 µs burst is shown in Fig. 8 (taken from [7]). Note: for applications involving tens of millijoules, more stages might be considered, for lower energies (µJ-level range) one to two OPCPA stages are sufficient.

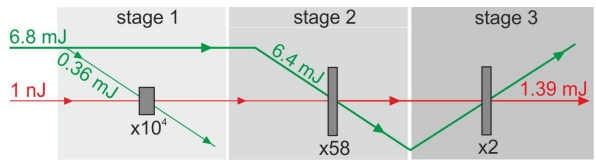

Figure 7: Schematic of a three-stage OPCPA: pump pulses (green) and signal pulses (red). As an example, energies and gains are taken from [7].

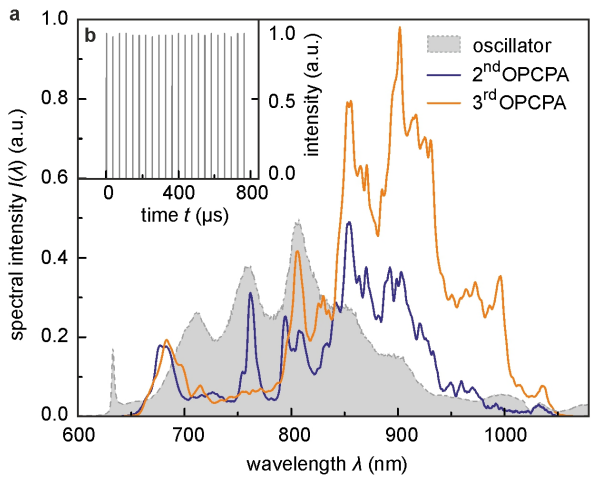

Figure 8: Three-stage broadband OPCPA [7]: (a) Spectral intensity of the Ti:sapphire oscillator (grey shaded), amplified spectra after the second (blue line) and third OPCPA stage (orange line). The amplified spectral bandwidth is $\Delta\nu = 168$ THz at $1/e^2$ ($\Delta\lambda = 360$ nm at $\lambda_c = 800$ nm), with a Fourier-limited pulse duration of 6.4 fs. (b) Inset: Typical pulse train during the burst-mode operation.

For a designer of a high power OPCPA system, one of the most important considerations is the pump-to-signal

ISBN 978-3-95450-133-5

conversion efficiency, because typically the pump amplifier dominates the costs of the complete system. As an example, an overall efficiency of 10.2% was achieved from the infrared pump to the signal output [7]. The contributions to this value were from the SHG and the three-stage OPCPA (see Fig. 7):

$$13.2\ \text{mJ} \xrightarrow{\text{SHG 51\%}} 6.8\ \text{mJ} \xrightarrow{\text{OPCPA 20\%}} 1.4\ \text{mJ}. \quad (3)$$

Power Scaling in Continuous Mode

The previous discussed results were carried out in burst mode. However, in continuous mode and at such high average powers, the linear absorption of optical power within the crystals cannot be neglected. This leads to inhomogeneous heating of the nonlinear optical crystal and results in spatial temperature changes. Spatially inhomogeneous refractive index changes can occur, which lead to spatially varying phase-matching conditions, limiting the attainable average power, the spectral bandwidth [29], and the beam quality [26]. Previously, the literature values for the linear absorption coefficients (α_{515}) at the OPCPA-pump wavelength at values near 515 nm were given as upper limit estimates: for example, $\alpha < 10^4$ ppm cm^{-1} at 532 nm for BBO, and $\alpha < 10^3$ ppm cm^{-1} at 532 nm for LBO [30]. Older techniques for measuring very small linear absorption coefficients were based on resonator methods, which suffer from misinterpreting scatter or reflection loss for absorption.

In a recent work [27], we have provided up-to-date measurements of the absorption coefficients at 515 nm using the photothermal common-path interferometry (PCI) method [31, 32]. The results demonstrate a large variation of absorption values within and on the surface of the crystals (for an example see Fig. 9 with an average absorption coefficient of 37.33 ppm cm^{-1} in volume). Additionally, in the case of BBO there would appear to be a large variation between manufacturers. Compared to older literature values, these new values are 1-2 orders of magnitude lower. There are two possible explanations for this discrepancy: (i) improved crystal growing and handling methods, and (ii) the accuracy of the PCI method. These new results show that for high power applications and for large bandwidth amplification, BBO and LBO are still the best crystals for these wavelengths. The application of BIBO for high powers is limited by two-photon absorption at 515 nm.

Another important consideration for high power OPCPA is the correct choice of the signal center frequency and bandwidth. Not only is it important to consider the absorption of the narrow band pump pulse, but the signal and idler pulses can also have significant contributions [29]. Figure 10 shows the optical transmission dependence on wavelength for both LBO and BBO; additionally, simulated signal spectra for LBO and BBO centered at 810 nm with a bandwidth supporting sub-7.0 fs (Fourier-limited) signal pulses and corresponding idler spectra are shown (taken from [26]). The idler spectrum is dependent on the pump wavelength and the broadband signal wavelengths through $1/\lambda_I = 1/\lambda_P - 1/\lambda_S$. In both cases, the signal spectrum must be cut off below

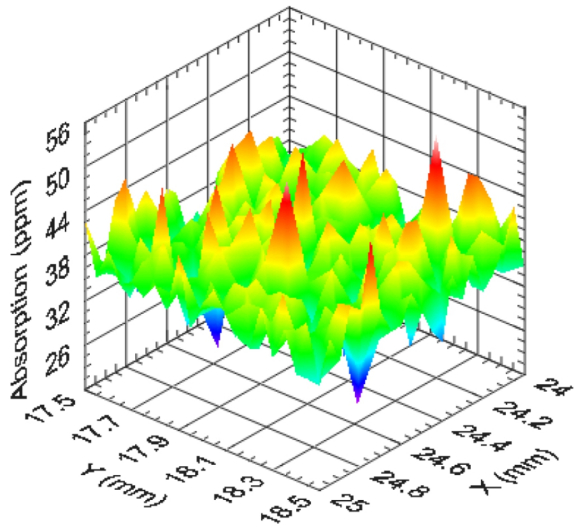

Figure 9: An example measurement of the volume absorption of an LBO sample using the common-path interferometry method (taken from [27]).

700 nm to prevent a strong idler infrared absorption within the range between 2000 and 3000 nm. Given the newly measured absorption coefficients and careful selection of the signal bandwidth, few-cycle laser pulses could be generated with above kW-level of average power [27]. A detailed discussion of thermal effects for high power OPCPA applications, including other parasitic waves, is given in [26, 27].

In order to demonstrate the flexibility of OPCPA and the power scaling limits, we realized a compact wavelength-tunable sub-30 fs amplifier with 11.4 W of average power with 20.7% pump-to-signal conversion efficiency at a repetition rate of 3.25 MHz [5]. The broadband signal was generated in a YAG crystal and the complete OPCPA setup was demonstrated on a bread board 80×80 cm^2. The OPCPA pump source was an Innoslab amplifier (AMPHOS, [33]). The OPCPA results are shown in Fig. 11. First, the OPCPA was optimized for broadband amplification. The average output power was 11.4 W (pulse energy of 3.5 µJ) with a spectrum supporting a Fourier-limited pulse of 6 fs FWHM (Fig. 11a). Second, a wavelength-tunable option was tested with a central wavelength between 700 and 900 nm (spectra shown in Fig. 11b). As an example, an autocorrelation measurement of a compressed pulse at center wavelength of 800 nm, with pulse duration of 29.1 fs FWHM was demonstrated (Fig. 11c). For more details see [5].

CONCLUSION

In this review, we discussed some of the technological developments for achieving high power OPCPAs pumped at 515 nm using Yb-doped solid-state lasers in both burst mode and continuous mode. These developments have important applications for high repetition rate FELs. Compared to Ti:sapphire amplifiers, OPCPA technology has a number of advantages. First, OPCPA is scalable to high powers [27];

ISBN 978-3-95450-133-5

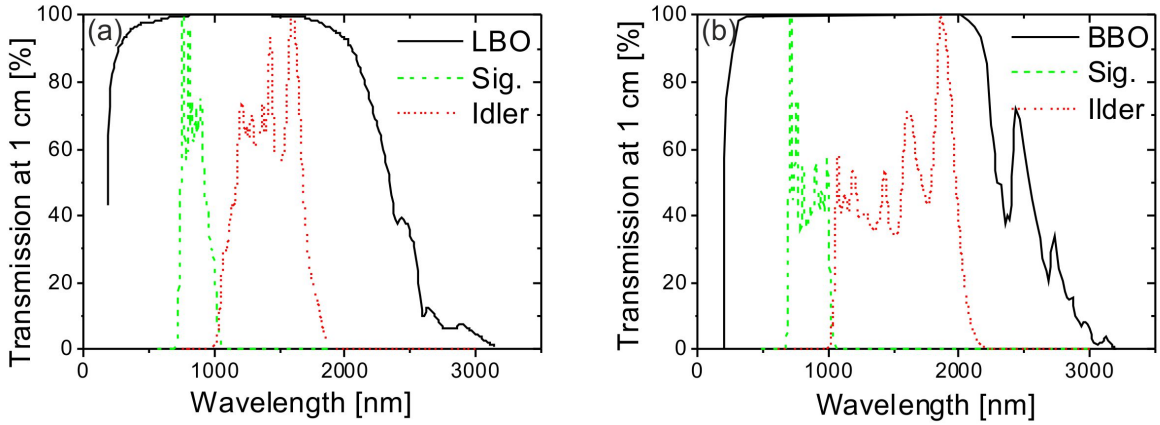

Figure 10: Optical transmission in dependence on wavelength [34], and spectra of signal and idler pulses at the end of the second stage for both LBO (a) and BBO (b) (taken from [26]).

second, OPCPA can amplify a broader bandwidth at high powers [5–7], thereby producing shorter pulses; and third, OPCPA is a wavelength tunable amplifier at high powers [5]. These new developments have been made possible by advances in Yb-doped solid-state laser technology, which also has the potential to be scalable to high powers. For example, 14 kW burst average power has been demonstrated from a 2-stage Yb:YAG thin-disk multipass amplifier [25]. Finally, since OPCPA does not require sophisticated cooling, it is possible to achieve a compact design, allowing reduced laboratory space and better stability [5].

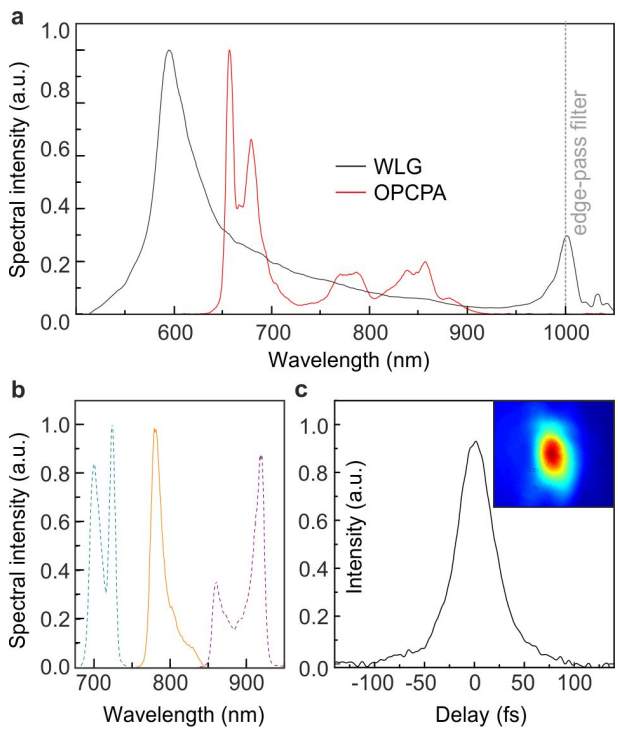

Figure 11: High-power OPCPA [5]: a) Broadband amplified signal (OPA, red) with $\Delta\lambda$ = 238 nm at 5% intensity maximum; WLG spectrum (WLG, grey line). b) Selected tunable narrow-band spectra between 700–900 nm, with $\Delta\lambda$ = 54 nm bandwidth at 10% intensity maximum. c) Autocorrelation (black line) at 800 nm (orange spectrum in (b)), with a pulse duration of 29.1 fs FWHM. Inset: amplified signal beam profile.

REFERENCES

[1] L. Lilje et al., "Achievement of 35 MV/m in the superconducting nine-cell cavities for TESLA", Nucl. Instr. Meth. Phys. Res. A **524**, 1–12 (2004).

[2] J. Feldhaus, "FLASH – the first soft x-ray free electron laser (FEL) user facility", J. Phys. B: At. Mol. Opt. Phys. **43**, 194002 (2010).

[3] B. Faatz et al., "Flash II: Perspectives and challenges", Nucl. Instr. Meth. Phys. Res. A **635**, S2–S5 (2011).

[4] H. Redlin et al., "The FLASH pump-probe laser system: Setup, characterization and optical beamlines", Nucl. Instr. Meth. Phys. Res. A **635**, S88–S93 (2011).

[5] R. Riedel et al., "Power scaling of supercontinuum seeded megahertz-repetition rate optical parametric chirped pulse amplifiers", Opt. Lett. **39**, 1422–1424 (2014).

[6] J. Rothhardt et al., "Octave-spanning OPCPA system delivering CEP-stable few-cycle pulses and 22 W of average power at 1 MHz repetition rate", Opt. Express **20**, 10870–10878 (2012).

[7] R. Riedel et al., "Long-term stabilization of high power optical parametric chirped-pulse amplifiers", Opt. Express **21**, 28987–28999 (2013).

[8] F. Tavella et al., "90 mJ parametric chirped pulse amplification of 10 fs pulses", Opt. Express **14**, 12822–12827 (2006).

[9] F. Tavella et al., "Fiber-amplifier pumped high average power few-cycle pulse non-collinear OPCPA", Opt. Express **18**, 4689–4694 (2010).

[10] J. Rothhardt et al., "High average and peak power few-cycle laser pulses delivered by fiber pumped OPCPA system", Opt. Express **18**, 12719–12726 (2010).

ISBN 978-3-95450-133-5

[11] M. Lenzner et al., "Sub-20-fs, kilohertz-repetition-rate Ti:sapphire amplifier", Opt. Lett. **20**, 1397–1399 (1995).

[12] A. Dubietis, G. Jonušauskas and A. Piskarskas, "Powerful femtosecond pulse generation by chirped and stretched pulse parametric amplification in BBO crystal", Opt. Commun. **88**, 437–440 (1992).

[13] I. N. Ross et al., "The prospects for ultrashort pulse duration and ultrahigh intensity using optical parametric chirped pulse amplifiers", Opt. Commun. **144**, 125–133 (1997).

[14] G. Cerullo and S. De Silvestri, "Ultrafast optical parametric amplifiers", Rev. Sci. Instrum. **74**, 1–18 (2003).

[15] R. Butkus et al., "Progress in chirped pulse optical parametric amplifiers", Appl. Phys. B **79**, 693–700 (2004).

[16] A. Dubietis, R. Butkus and A. P. Piskarskas, "Trends in chirped pulsed optical parametric amplification", IEEE J. Sel. Topics. Quantum Electron. **12**, 163–172 (2006).

[17] B. C. Stuart et al., "Laser-induced damage in dielectrics with nanosecond to subpicosceond pulses", Phys. Rev. Lett. **74**, 2248–2251 (1995).

[18] M. Schulz et al., "Yb:YAG Innoslab amplifier: efficient high repetition rate subpicosecond pumping system for optical parametric chirped pulse amplification", Opt. Lett. **36**, 2456–2458 (2011).

[19] M. Schulz et al., "Pulsed operation of a high average power Yb:YAG thin-disk multipass amplifier", Opt. Express **20**, 5038–5043 (2012).

[20] M. Bradler, P. Baum and E. Riedle, "Femtosecond continuum generation in bulk laser host materials with sub-μJ pump pulses", Appl. Phys. B **97**, 561–574 (2009).

[21] T. Eidam et al., "Femtosecond fiber CPA system emitting 830 W average output power", Opt. Lett. **35**, 94–96 (2010).

[22] J. Limpert et al., "Performace Scaling of Ultrafast Laser Systems by Coherent Addition of Femtosecond Pulses", IEEE J. Sel. Topics Quantum Electron. **20**, 0901810 (2014).

[23] P. Russbueldt et al., "Compact diode-pumped 1.1 kW Yb:YAG Innoslab femtosecond amplifier", Opt. Lett. **35**, 4169–4171 (2010).

[24] A. Giesen and J. Speiser, "Fifteen Years of Work on Thin-Disk Lasers: Results and Scaling Laws", IEEE J. Sel. Topics Quantum Electron. **13**, 598–609 (2007).

[25] M. Schulz et al., "14 kilowatt burst average power from 2-stage cascaded Yb:YAG thin-disk multipass amplifier", in Frontiers in Optics 2013, I. Kang, D. Reitze, N. Alic, and D. Hagan, eds., OSA Technical Digest (Optical Society of America, 2013), paper FTu4A.2. http://www.opticsinfobase.org/abstract.cfm?URI=FiO-2013-FTu4A.2

[26] M. J. Prandolini et al., "Design considerations for a high power, ultrabroadband, optical parametric chirped-pulse amplifier", Opt. Express **22**, 1594–1607 (2014).

[27] R. Riedel et al., "Thermal properties of borate crystals for high power optical parametric chirped-pulse amplification", Opt. Express **22**, 17607–17619 (2014).

[28] Z. M. Liao et al., "Energy and average power scalable optical parametric chirped-pulse amplification in yttrium calcium oxyborate", Opt. Lett. **31**, 1277–1279 (2006).

[29] J. Rothhardt et al., "Thermal effects in high average power optical parametric amplifiers", Opt. Lett. **38**, 763–765 (2013).

[30] D. N. Nikogosyan, *Nonlinear Optical Crystals: A Complete Survey* (Springer Science+Business Media, Inc., 2005).

[31] A. Alexandrovski et al., "Photothermal common-path interferometry (PCI): new developments", Proc. SPIE 7193, Solid State Lasers XVIII: Technology and Devices, 71930D (2009); doi:10.1117/12.814813.

[32] B. Gronloh et al., "Green sub-ps laser exceeding 400 W of average power", Proc. SPIE 8959, Solid State Lasers XXIII: Technology and Devices, 89590T (2014); doi:10.1117/12.2041288.

[33] T. Mans et al., "Highly flexible ultrafast laser system with 260 W average power", Proc. SPIE 7912, Solid State Lasers XX: Technology and Devices, 79120M (2011); doi: 10.1117/12.874417.

[34] A.V. Smith, *SNLO nonlinear optics code (Ver. 60)*, AS-Photonics, Albuquerque, USA (2013).

ISBN 978-3-95450-133-5